Seismic Dynamic Response Analysis of Soil Rock Binary Structure Slopes——A Case Study of Pusaxi Slope in Sichuan

Yunfei Zhang[1], Kun Wang[1*], Jingkun Bao[2], Taiqiang Yang[3], Junyao Luo[3]

[1] Faculty of Civil Engineering and Mechanics, Kunming University of Science and Technology, Kunming 650500, China
[2] Faculty of Land Resources Engineering, Kunming University of Science and Technology, Kunming 650221, China
[3] Power China Kunming Engineering Corporation Limited, Kunming 650032, China
kmwk2016@kust.edu.cn

Abstract. The frequent occurrences of earthquakes often pose serious threats to the stability of geological engineering structures in the affected areas. This article takes the Pusaxi side slope in Sichuan Province as an example, this study utilizes Geo-studio numerical simulation software to conduct comprehensive dynamic response analysis of slopes. The research aims to investigate the dynamic response patterns and stability of slopes under seismic actions. Parameters such as displacement, velocity, acceleration, and acceleration amplification factor are analyzed to determine the dynamic response of slopes. The study reveals that the displacement response of slopes correlates positively with the amplitude of seismic waves. Acceleration response indicates that the bottom of the slope tends to fail earlier than the upper parts under earthquake conditions. Internal dynamic responses of slopes exhibit elevation amplification effects and slope surface amplification effects. Analysis of displacement, velocity, acceleration, and acceleration amplification factor shows that the strongest dynamic response of slopes occurs at approximately half the elevation of the slope surface. Stability calculations using Newmark permanent displacement suggest that slopes are prone to failure when earthquakes exceed magnitude 5.

Keywords: Slope stability; Geo-Studio; Dynamic response; Acceleration amplification coefficient; Newmark Permanent displacement

1 Introduction

Earthquake-induced landslides are a common secondary hazard of earthquakes, posing a significant threat to people's livelihoods[15]. Therefore, slope stability has been a hot topic of research both domestically and internationally[2]. Globally, China is among the countries most severely affected by earthquakes and their secondary hazards. In the western regions of China, including Yunnan, Guizhou, Sichuan, and

W. Guo et al. (eds.), *Proceedings of the 3rd International Conference on Green Building, Civil Engineering and Smart City (GBCESC 2024)*, Advances in Engineering Research 264,
https://doi.org/10.2991/978-94-6463-728-1_35

Chongqing, earthquake disasters frequently occur. The Wenchuan earthquake in Sichuan in 2008 (ML=8.0) triggered approximately 56,000 landslides and rock collapses, creating over 10,000 potential earthquake disaster sites[11].

Zhang Bin et al[7] studied the dynamic response and seismic subsidence deformation of slopes in loess hilly areas under earthquake action.Zhang Bin et al[13]conducted research on the dynamic response and seismic settlement deformation analysis method of slopes in loess hilly areas.Gu Kunsheng et al[9]studied the dynamic response law and spectral characteristics of anti dipping rock slopes under earthquake action.Xu Ming et al[12]studied the seismic dynamic response and failure mode of inclined layered fractured rock slopes. Ma Enshuai et al[6]analyzed the effects of earthquake intensity and reservoir water level changes on slopes using Geo-studio software. Liu Yi[5]simulated the process of earthquake impact on slopes considering pore water pressure based on the mechanism of retaining walls. Yang Bing et al.[14]studied the process and dynamic response of seismic-induced crack-slip type slope failures using a large-scale shaking table. Wang Lanmin et al[10]conducted shaking table tests on loess slopes under the combined effect of earthquakes and rainfall. Chen Jipu[1]analyzed the dynamic response of tailings dams under seismic action using both model tests and numerical simulations. Liu Hanxiang et al[4]researched the dynamic characteristics of layered composite rock slopes using a shaking table. Wang Bendong et al[8]studied slope stability using the Newmark permanent displacement method.

This paper, combined with specific engineering cases, uses numerical simulation to study the dynamic response and stability of soil-rock dual structure slopes under seismic action. It presents the dynamic response patterns of the slopes and their stability under different seismic magnitudes.

2 Site Overview

2.1 Natural Geography and Project Overview

The Pusaxi landslide is located in Xiaopuzi Village, Eryi Town, Jiulong County, Ganzi Prefecture, southeast of Jiulong County, 52 km away from the county seat, covering an area of 116 km². It is about 600 km from Chengdu, with convenient transportation connected by township roads and the Beijing-Kunming Expressway. The geographical coordinates of the slope are: 101 ° 55'5.47"~101 ° 55'9.53"E longitude, 28°42'16.48"~28°42'17.49"N latitude.

Detailed on-site investigations revealed that the slope developed within the Quaternary loose accumulation layer as a soil landslide. According to geological mapping, drilling, and trenching, the original strata of the Pusaxi landslide are Quaternary Holocene residual slope deposits, including colluvial and alluvial soils. The soil types in the colluvial layer are blocky soil and gravelly soil, distributed throughout the landslide area, slightly moist to moist, mainly composed of blocks, gravel, and sandy soil, slightly dense to medium dense. The loose deposits of different origins are distributed differently: man-made fill (Q_4^{ml}) is found in front of the farm roads and residential houses, mainly composed of silt and gravel soil. Colluvial loose deposits (Q_4^{el+dl}) are mainly distributed in gentle slope areas, consisting of blocky soil, weakly cemented.

Jiulong County has been recording fixed observations of earthquakes since January 1984. In the 1990s, small earthquakes of magnitude 2 to 4 frequently occurred within the county, with epicenters concentrated in the eastern Dacheng Mountain core area and the western Yalong River area, while the central Jiulong River valley remained relatively stable. On February 23, 2003, a magnitude 6.0 earthquake occurred at the junction of Ya (Jiang) - Jiu (Long) - Kang (Ding). According to the Chinese seismic zoning map (GB18306-2001), earthquakes are a major factor inducing geological disasters in Jiulong County.

2.2 Current Status of the Slope

The slope is located in the southern slope area, with the landslide front connected to the township road, and the rear edge of the landslide body is a residential area and hydropower station pressure pipeline. The slope body is partially farmland, with villagers using block stones to build simple retaining walls in farmland and residential areas. The slope area elevation ranges from 2085 to 2163 m, with a relative height difference of 78 to 100 m, and a slope of 26° to 40°, with the middle and front parts of the slope being steeper. The overall shape of the slope is semi-circular, with a longitudinal length of 129 m, a front edge width of 65 m, a rear edge width of 83 m, and an area of approximately 10,368 m^2. The thickness of the soil layer is about 7 to 11 m, with a predicted volume of 83,000 m^3, classified as a small soil landslide.

3 Numerical Simulation Calculations

3.1 Model Establishment

Geo-Studio software developed by GEO-SLOPE International Ltd. in Canada was used to simulate the dynamic response of three cross-sections (Figure 1) of the entire slope. Based on borehole wave velocity test results and the physical and mechanical properties of the site's soil and rock, the strata were simplified into two types of materials: ① clay, ② basalt. The physical and mechanical parameters of the two media in the model are shown in Table 1.

Table 1. Physical and mechanical parameters of different.

Rock Layer	Unit Weight (kN/m^3)	Poisson's Ratio	Cohesion (kPa)	Friction Angle (°)
Clay	19	0.21	20	28
Basalt	28	0.24	42	45

The calculation used the Mohr-Coulomb model, combining the slope/w and quake/w modules of Geo-Studio. The former is used for static stability analysis of the slope under natural conditions, and the latter is mainly used for dynamic response analysis. Modeling was done on the three sections mentioned, with bottom elevations of 2070 m, 2070 m, and 2075 m for sections 1-1, 2-2, and 3-3 respectively. Automatic mode was used for grid division, with 1834 grid elements and 1749 nodes for section 1-1, 2081 grid elements and 2000 nodes for section 2-2, and 1998 grid elements and 2077 nodes for section 3-3. The dynamic response of the slope was studied by introducing the acceleration amplification factor, which is the ratio of the peak acceleration of the monitoring point to the peak input acceleration, as well as the displacement and acceleration response of the slope surface. Stability analysis was conducted using Newmark permanent displacement method.

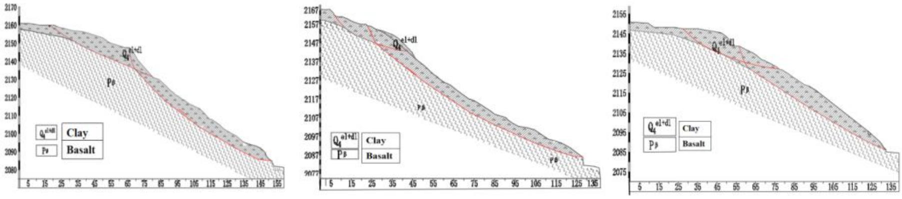

(a)Cross-Section 1-1 (b) Cross-Section 2-2 (c)Cross-Section 3-3

Fig. 1. Geometric schematic diagram of landslide sections 1-1, 2-2, 3-3

Two horizontal monitoring lines (H1-1, H1-2, H2-1, H2-2, H3-1, H3-2) and two vertical monitoring lines (V1-1, V1-2, V2-1, V2-2, V3-1, V3-2) were set up within each of the three cross-sections. Five monitoring points were set on the slope surface of each section, as shown in Figure 2.

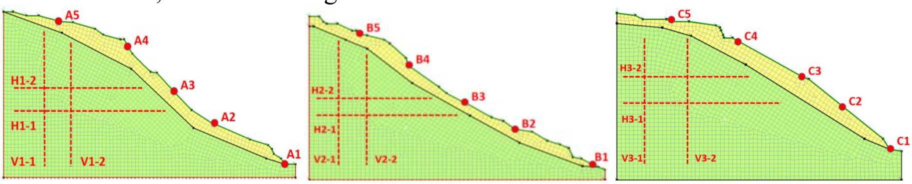

(a)Cross-Section 1-1 (b) Cross-Section 2-2 (c)Cross-Section 3-3

Fig. 2. Calculation models and monitoring point arrangements for three cross-sections

3.2 Seismic Waves

To simulate the impact of seismic parameters on the dynamic response of the slope, an El-Centro wave with a 10% probability of exceedance in 50 years was used. The El-Centro wave was adjusted for different amplitudes and time compression ratios to simulate the effects of amplitude and frequency. The acceleration time history curve of the El-Centro wave is shown in Figure 3. The seismic fortification intensity for the calculation area is 7 degrees, with a design basic acceleration value of 0.313g. The seismic wave action time was set to 15 seconds, with a decay time of 5 seconds.

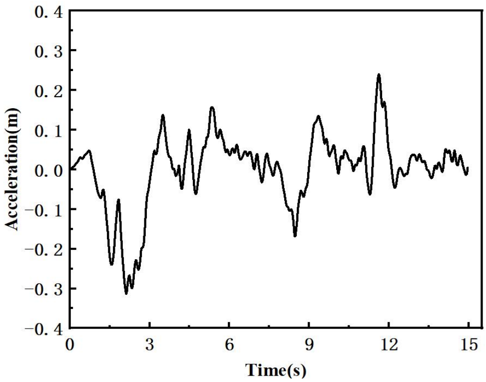

Fig. 3. Seismic wave acceleration time history curve

4 Analysis of Calculation Results

4.1 Analysis of Dynamic Response Characteristics

Displacement Response Characteristics Analysis. Figure 4 shows the displacement at different elevations on the slope surface. Combining the displacements observed on the slope surfaces of the three sections, it can be seen that under seismic action, the displacement on the slope surface does not increase with elevation. Instead, it reaches a maximum at approximately half the total height of the slope and then gradually decreases. This indicates that the dynamic response is most intense at the midpoint elevation of the slope surface.

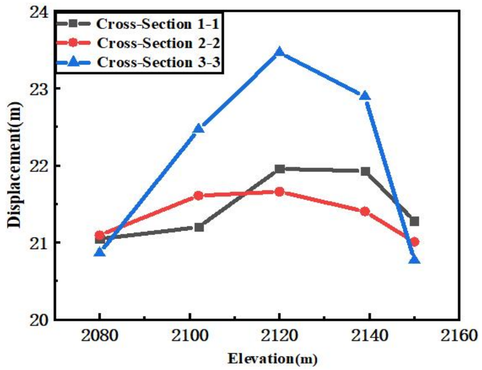

Fig. 4. Displacement of monitoring points on slope surfaces of sections 1-1, 2-2, and 3-3 at different elevations

Figure 5 shows the displacement of different monitoring points on the slope surface of the three sections under varying amplitude intensities. It can be observed that there is a positive correlation between amplitude and the displacement of the monitoring points, meaning that the displacement of the slope surface increases with the intensity of the amplitude. However, the response of the five monitoring points on each section to the same amplitude varies. For example, under an amplitude of 0.5 g, the displacements of monitoring points A3 and A4, located in the middle of the slope on section 1-1, are significantly greater than those of the other three monitoring points. Similarly, the displacements of the central slope monitoring points on the other two sections are greater than those of the other monitoring points on the same section. The displacement response of the monitoring points on the slope surfaces of the three sections under different amplitudes shows the same characteristic, indicating that, in terms of displacement, the middle of the slope responds most intensely under seismic action.

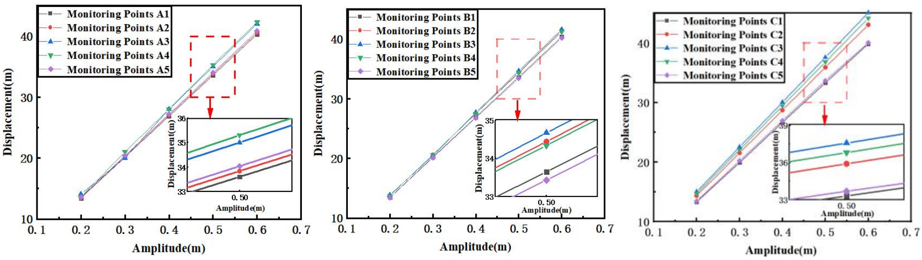

(a)Cross-Section 1-1 (b)Cross-Section 2-2 (c)Cross-Section 3-3

Fig. 5. Displacement of monitoring points on slopes of sections 1-1, 2-2, and 3-3 under different amplitudes

Analysis of Velocity Response Characteristics. The figure 6 below shows the variation of velocity with elevation at monitoring points on the slope surfaces of sections 1-1, 2-2, and 3-3. It can be seen that under seismic action, the velocity on the slope surface first increases and then decreases with elevation, reaching a maximum at approximately half the total height of the slope. This indicates that the velocity response is most intense at the midpoint elevation of the slope surface. Both the velocity and displacement response patterns indicate that the dynamic response of the slope is most intense at half the slope height. To verify this pattern, the following sections will study the acceleration and acceleration amplification factors.

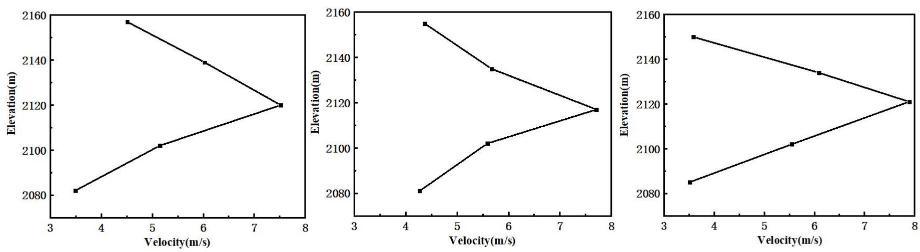

(a)Cross-Section 1-1 (b) Cross-Section 2-2 (c)Cross-Section 3-3

Fig. 6. Displacement of monitoring points on slopes of sections 1-1, 2-2, and 3-3 under different amplitudes

Analysis of Acceleration Response Characteristics. Figures 7~9, and 11 respectively show the acceleration response at five monitoring points on the slope surfaces of sections 1-1, 2-2, and 3-3. It can be seen that with increasing elevation, the arrival time of the acceleration response peak is delayed. Specifically, for section 1-1, the times from A1 to A5 are 2.34s, 3.18s, 3.94s, 5.84s, and 6.00s, respectively; for section 2-2, the times from B1 to B5 are 2.40s, 3.16s, 3.76s, 5.56s, and 12.08s, respectively; and for section 3-3, the times from C1 to C5 are 2.64s, 3.46s, 4.08s, 5.86s, and 11.92s, respectively. Additionally, the peak displacement arrival times for points A1, B1, and C1 are later than the peak acceleration of the input seismic wave, indicating that there is a certain lag in the transmission of seismic energy through the slope.

Additionally, considering the peak acceleration values at the monitoring points on each section's slope surface, the peak acceleration responses at points A3, B3, and C3 are the highest among the five monitoring points on sections 1-1, 2-2, and 3-3, respectively. This phenomenon further indicates that the response is most intense at approximately half the total height of the slope under seismic action.

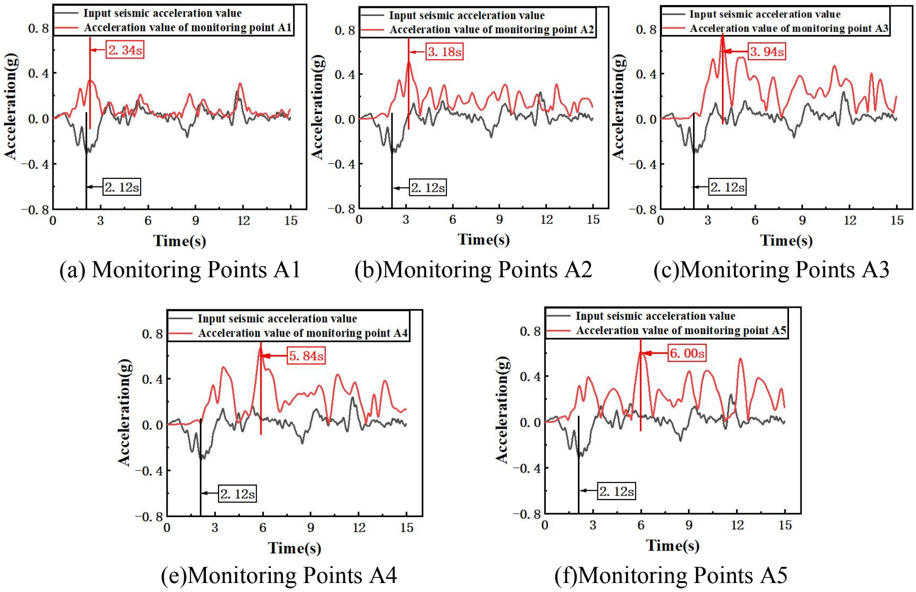

(a) Monitoring Points A1 (b)Monitoring Points A2 (c)Monitoring Points A3

(e)Monitoring Points A4 (f)Monitoring Points A5

Fig. 7. Time history diagram of acceleration at each monitoring point on the broken surface of section 1-1

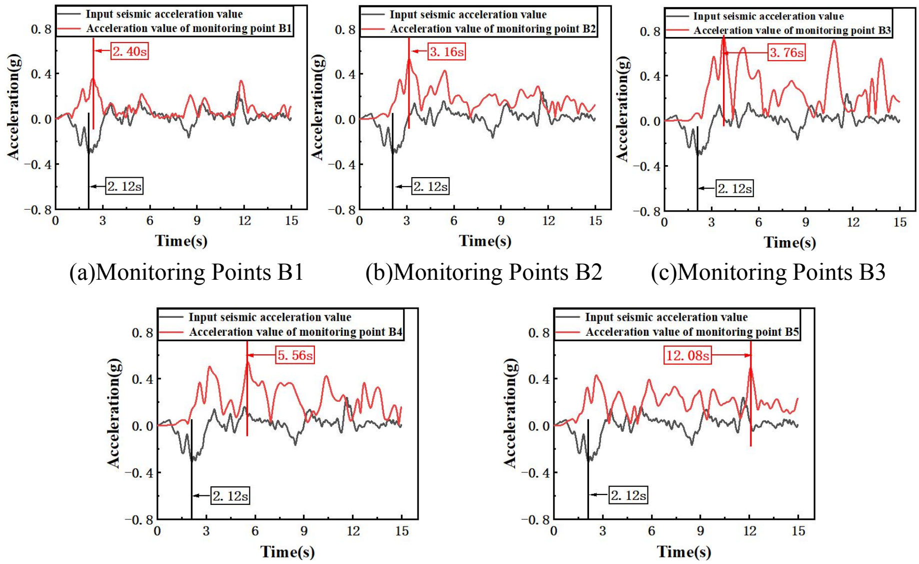

(a)Monitoring Points B1 (b)Monitoring Points B2 (c)Monitoring Points B3

(e)Monitoring Points B4 (f)Monitoring Points B5

Fig. 8. Time history diagram of acceleration at each monitoring point on the broken surface of section 2-2

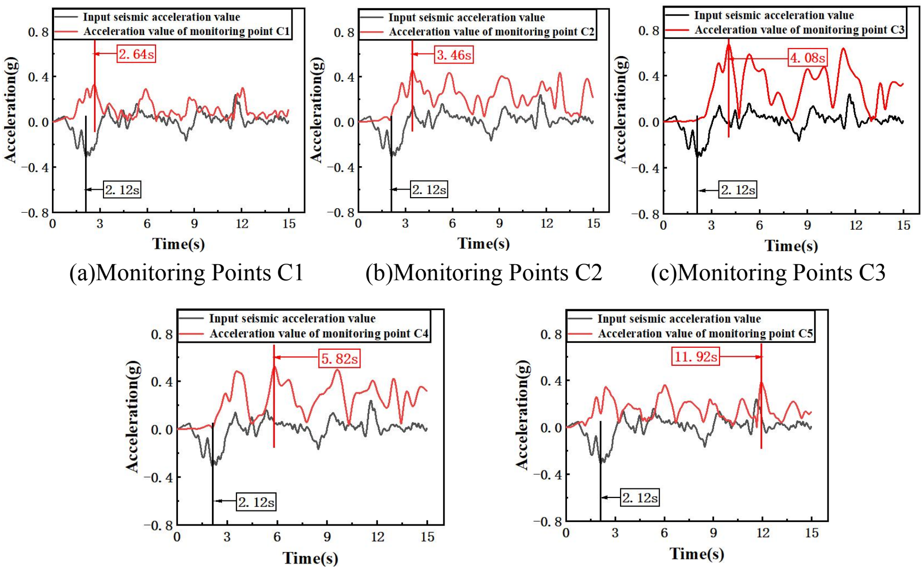

(a)Monitoring Points C1 (b)Monitoring Points C2 (c)Monitoring Points C3

(e)Monitoring Points C4 (f)Monitoring Points C5

Fig. 9. Time history diagram of acceleration at each monitoring point on the broken surface of section 3-3

Analysis of Acceleration Response Characteristics. This section uses the acceleration amplification factor, defined as the ratio of the peak acceleration of the dynamic response to the peak input acceleration, to study the dynamic response of the slope. First, the internal conditions of the slope are investigated. Figure 10 shows the variation of the acceleration amplification factor with elevation along vertical monitoring lines inside the slope for the three sections. In each section, two vertical monitoring lines are selected, and ten monitoring points are evenly distributed along each line. The relative elevation is expressed as the value obtained by dividing the elevation of the monitoring point (h) by the height of the monitoring line (H). As shown in Figure 10, the acceleration amplification factor along the vertical monitoring lines inside the slope increases with elevation, indicating that the dynamic response of the slope in the vertical direction has an "elevation amplification effect."

In the slope, there are also two horizontal monitoring lines to demonstrate the variation of the acceleration amplification factor in the horizontal direction. Ten points are evenly selected along each monitoring line as monitoring points. The relative distance is calculated by dividing the distance (d) from the monitoring point to the left boundary by the length (D) of the monitoring line. As shown in Figure 11, the acceleration amplification factor of the monitoring points significantly increases with the distance from the left boundary. This is especially evident in sections 1-1 and 2-2, which exhibit an almost linear positive correlation. This indicates that the closer to the slope surface in the horizontal direction within the slope, the stronger the dynamic response, illustrating the "slope surface amplification effect" in the horizontal direction within the slope.

The above results indicate that the acceleration response on the slope surface is greater than that within the slope. By extracting the acceleration amplification factor values from the monitoring points on the slope surfaces of the three sections (Figure 12), it can be seen that the acceleration amplification factor of the monitoring points on the slope surface first increases and then decreases with elevation, reaching a maximum at approximately half the total height of the slope. This shows that, regardless of displacement response, acceleration response, or acceleration amplification factor, the response is most intense at half the slope height under seismic action.

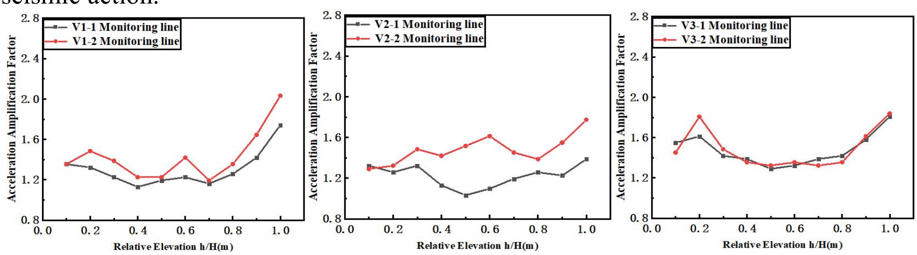

(a)Cross-Section 1-1 (b) Cross-Section 2-2 (c)Cross-Section 3-3

Fig. 10. Vertical Acceleration Amplification Coefficient of Landslides in Sections 1-1, 2-2, 3-3 as a Function of Elevation

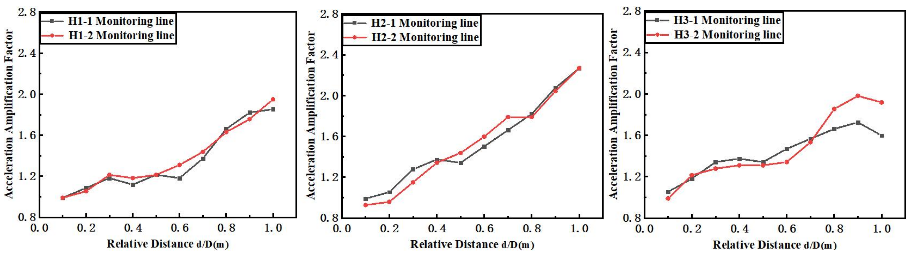

(a)Cross-Section 1-1 (b) Cross-Section 2-2 (c)Cross-Section 3-3

Fig. 11. Variation of Horizontal Acceleration Amplification Coefficient with Distance in Sections 1-1, 2-2, 3-3 Landslides

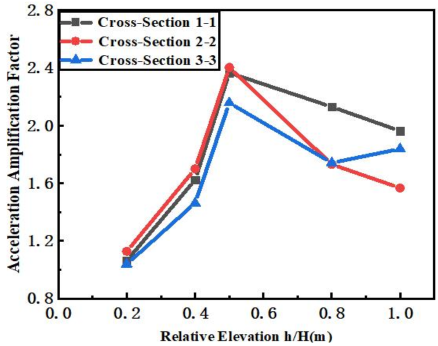

Fig. 12. Acceleration amplification coefficient of monitoring points on the surface of landslides at sections 1-1, 2-2, 3-3 as a function of elevation

4.2 Analysis of Slope Stability Based on Newmark Permanent Displacement

When using the Newmark method to calculate permanent displacement, the slope should have a clearly defined sliding surface, which is typically identified using the limit equilibrium method for the static critical sliding surface. Newmark assumes that each sliding block has a constant yield acceleration- a_y , during sliding. The block will only slide when the seismic acceleration exceeds this yield acceleration. By performing a double time integration of the seismic acceleration that exceeds the yield acceleration, the cumulative permanent displacement U of the slope under seismic action can be obtained(Figure 13). Namely:

$$U = \quad [a(t) - a_y]dt \tag{1}$$

In the equation, $a(t)$ represents the acceleration of the sliding mass, and(t)denotes the time when the acceleration exceeds the yield acceleration.

Now, the probability of failure equation given by Jibson et al. (1998) is used to determine the stability of the slope. The equation is as follows[3]:

$$P_f = 0.335[1 - exp(- 0.048U^{1.565})] \tag{2}$$

In the formula: P_f is the failure probability; U is the permanent displacement, measured in centimeters.

Jibson and others provided an estimation of slope instability probability using this formula:

1. When Newmark displacement is 0-1 cm, the probability of slope instability is low (0%-2%).
2. When Newmark displacement is 1-5 cm, the probability of slope instability is moderate (2%-15%).
3. When Newmark displacement is 5-15 cm, the probability of slope instability is high (15%-32%).
4. When Newmark displacement is greater than 15 cm, the probability of slope instability is very high (>32%).

This section uses section 1-1 as an example to demonstrate the Newmark permanent displacement method. 1) First, a static analysis of the slope is performed to obtain a critical slip surface. 2) Under seismic conditions, a scatter plot of acceleration versus slope safety factor for the slip surface is generated, and the Fs-a curve is fitted. The yield acceleration is taken as ($a_y = 0.0578 m^2/s$) when the safety factor is 1. 3) The permanent displacement is obtained by subtracting the yield acceleration from the existing acceleration time history curve and performing a double integration.To study the stability of the slope under different seismic conditions, this paper calculates the permanent displacements corresponding to different earthquake magnitudes and assesses failure. According to the "Slope Engineering Safety Code," the peak acceleration of seismic waves corresponds to different earthquake magnitudes. Therefore, the peak accelerations of seismic waves are taken as 0.05g, 0.2g, and 0.313g, corresponding to magnitude 5, 6, and 7 earthquakes, respectively. Following the process shown in Figure 13, the permanent displacements for the three sections under these three seismic conditions were calculated, and the results are presented in Table 2. As seen from Table 2, when the slope is subjected to a magnitude 5 earthquake, the permanent displacement is 0 cm. However, when the earthquake magnitude exceeds 5, the permanent displacement of the slope generally exceeds 15 cm, indicating a high probability of instability. Therefore, the slope is expected to remain stable under earthquakes of magnitude 5 and below.

Table 2. Permanent displacement under different magnitudes

Cross-Section	Permanent displacement due to a magnitude 5 earthquake (m)	Permanent displacement due to a magnitude 6 earthquake (m)	Permanent displacement due to a magnitude 7 earthquake (m)
1-1	0	0.368362	2.71275
2-2	0	0.130711	1.20997
3.3	0	1.7152	9.3066

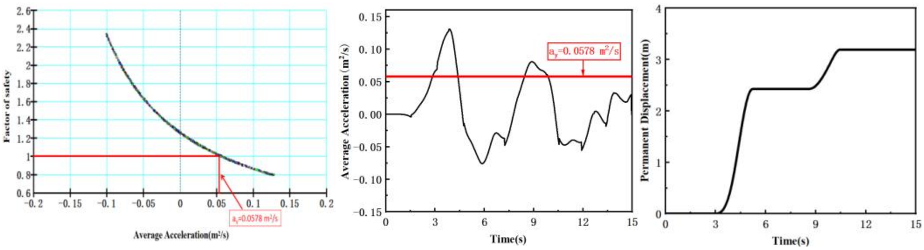

(a)Fs-a curve (b)acceleration time history curve (c)permanent displacement time history curve

Fig. 13. Section 1-1 Permanent Displacement Calculation

5 Conclusion

The following six conclusions can be drawn from the research in this article.

1.Under seismic conditions, with varying excitation intensity, there is a significant change in peak displacement response. As excitation intensity increases, the peak displacement on the slope surface gradually increases, indicating a positive correlation between peak displacement response and excitation intensity.

2. Through the study of acceleration time-history curves at slope monitoring points, it was found that the dynamic response of the slope does not occur simultaneously. As the elevation of the monitoring points increases, the time of occurrence of peak acceleration delays, indicating that the lower part of the slope fails earlier than the upper part.

3. The degree of dynamic response of the slope varies in different parts of the slope. The amplification factor of acceleration in the vertical direction inside the failed mass increases with elevation, showing a "elevation amplification effect" of slope dynamic response; in the horizontal direction, closer distances to the slope surface result in larger acceleration amplification factors, indicating a "surface amplification effect" of slope dynamic response.

4. This study comprehensively investigates the response of displacement, velocity, acceleration, and acceleration amplification factors of slopes under seismic action. It was found that the strongest dynamic response of the slope under seismic conditions occurs at half the elevation of the slope surface. Therefore, the most dangerous part of the slope under seismic conditions is the central part of the slope surface. To enhance the seismic resistance of the slope, emphasis should be placed on reinforcing the central part of the slope surface, in addition to conventional protection measures.

5. Through permanent displacement analysis using Newmark method, the stability of slopes under seismic action was analyzed. It was found that stability may be maintained under earthquakes of less than magnitude 5, while slopes are generally damaged under earthquakes of magnitude greater than 5.

Additionally, this study has its limitations. The conclusions drawn from this specific case study provide significant guidance for other slopes with similar geological conditions and seismic environments. However, their applicability is limited for slopes with vastly different engineering geological conditions. To enhance the generalizability of the research findings, future studies should include a wider variety of geological and engineering environments, utilizing different parameter sets and model configurations to further validate the effectiveness of these results under various conditions.

Acknowledgement

This work is supported by Yunnan Fundamental Research Projects (Grant No. 202301AU070022)

References

1. Chen J P. Research on the Characteristics of Seismic Dynamic Responses of Tailings Pond Based on Numerical Simulation and Model Test.Kunming University of Science and Technology, (2015)
2. Gao Y F,Wang Y J,Zhang F, et al. State-of-the-art review on slope and embankment dams.China Civil Engineering Journal, 1-22, [2024-07-05], (2024).
3. Jibson R W, Harp, E L, Michael J A. A method for producing digital probabilistic seismic landslide hazard maps: An example from the Los Angeles.California, area: U. S. Geological Survey Open - File Report, 98 - 113, 17 p., 2 pl., Scale 1: 24,000, (1998).
4. Liu H X,Zhou Y F,Li X, et al. Shaking table test of dynamic responses of a layered complex rock slope under earthquake. Chinese Journal of Rock Mechanics and Engineering, 40 (04): 676-689, (2021).
5. Liu Y. Slope Stability Analysis of Masonry Retaining Wall Considering Pore Water Pressure and Earthquake Action Kunming University of Science and Technology, (2019).
6. Ma E S,Cheng J J,Liu Y, et al. Stability Analysis of Reservoir Slope under Earthquake Based on Quake/W Coupled with Slope/W——A Case study of Xiaoxiboti.Reservoir Journal of Shihezi University(Natural Science),(2015).
7. Huang Z Q,Li J L;Wang C, et al. Study on Dynamic Response and Failure Mode of Steep Bedding Rock Slope Under Strong Earthquake.Journal of Engineering Geology, 31 (01): 217-227, (2023).
8. Wang B D,Li S Q,Xu W Z, et al. Comparative Study on the Safety Factor Method of Reinforced Slope Based on Newmark Method.Journal of Geological Hazards and Environment Preservation, 34 (01): 64-70, (2023).
9. Gu K S,Guo M Z;Tang X W, et al.Dynamic Response and Spectrum Characteristics of Anti-dip Rock Slopes Under Earthquake.China Earthquake Engineering Journal, 44 (01): 62-71, (2022).
10. Wang L M;Pu X W;Wu Z J; et al.2017.The shaking table test of the instability sliding of loess slope under the coupling effects of earthquake and rainfall.Chinese Journal of Rock Mechanics and Engineering, 36(S2): 3873-3883, (2017).
11. Wu S B,Wang L Q,Wu Q, et al. Advance and Prospect for Seismic Dynamic Response of Anchored Rock Slope. Earth Science, 47 (12): 4456-4468, (2022).
12. Xu M;Yu X Y;Zhao Y P, et al. Analysis of Seismic Dynamic Response and Failure Mode of Bedding Rock Slope With Laminated Fractured Rock and Soil Mechanics, 44 (02): 362-372, (2023).

13. Zhang B;Shao S;Shao S J, et al.Dynamic Response of Slopes in Hilly Regions of Loess and Analysis Method for Their Seismic Subsidence Deformation.Chinese Journal of Geotechnical Engineering, 45 (04): 869-875, (2023).
14. Yang B,Yang X,Yang T, et al. Shaking table model test on dynamic response and failure process of shatter-burst sliding slope under earthquake load. Chinese Journal of Rock Mechanics and Engineering, 37(S1): 3279-3290, (2018).
15. Zeng X.Analysis of Anti-sliding Pile Supporting Slop Stability during Earthquake.Southwest Jiaotong University,(2017).